Hindawi Publishing Corporation
Mathematical Problems in Engineering
Volume 2015, Article ID 608015, 15 pages
http://dx.doi.org/10.1155/2015/608015

Research Article

Motion Control Design for an Omnidirectional Mobile Robot Subject to Velocity Constraints

Ollin Peñaloza-Mejía,[1] Luis A. Márquez-Martínez,[2] Joaquín Alvarez,[2] Miguel G. Villarreal-Cervantes,[3] and Ramón García-Hernández[1,4]

[1] *Departamento de Ingeniería Eléctrica y Electrónica, Instituto Tecnológico de Sonora, Campus Náinari, Antonio Caso 2266, Villa ITSON, 85130 Ciudad Obregón, SON, Mexico*
[2] *Departamento de Electrónica y Telecomunicaciones, CICESE, Carretera Ensenada-Tijuana No. 3918, Zona Playitas, 22860 Ensenada, BC, Mexico*
[3] *Departamento de Posgrado, CIDETEC, Instituto Politécnico Nacional, Sección de Mecatrónica, Juan de Dios Bátiz s/n, Nueva Industrial Vallejo, Gustavo A. Madero, 07700 México, DF, Mexico*
[4] *Universidad Autónoma del Carmen, Facultad de Ingeniería, Calle 56 No. 4, Benito Juárez, 24180 Ciudad del Carmen, CM, Mexico*

Correspondence should be addressed to Joaquín Alvarez; jqalvar@cicese.mx

Received 31 October 2014; Revised 8 February 2015; Accepted 15 February 2015

Academic Editor: Nazim I. Mahmudov

Copyright © 2015 Ollin Peñaloza-Mejía et al. This is an open access article distributed under the Creative Commons Attribution License, which permits unrestricted use, distribution, and reproduction in any medium, provided the original work is properly cited.

A solution to achieve global asymptotic tracking with bounded velocities in an omnidirectional mobile robot is proposed in this paper. It is motivated by the need of having a useful in-practice motion control scheme, which takes into account the physical limits of the velocities. To this end, a passive nonlinear controller is designed and combined with a tracking controller in a negative feedback connection structure. By using Lyapunov theory and passivity tools, global asymptotic tracking with desired bounded velocities is proved. Simulations and experimental results are provided to show the effectiveness of the proposal.

1. Introduction

Control of mobile robots has received great attention in last decades. The interest is motivated by the different potential applications in which these systems are very useful (e.g., indoor/outdoor navigation in wide areas). The fundamental control problems addressed have been regulation and trajectory tracking, and several control techniques have been proposed to successfully solve them (see, e.g., [1]). Also, the demands for mobile robots with high mobility have increased in the last years. Since the conventional mobile robot does not have high mobility due to its nonholonomic constraint, the omnidirectional mobile robot (OMR) has attracted the attention, because of its ability to move simultaneously, and independently in an arbitrary direction in the horizontal plane (translational motion) and with different orientation (rotational motion). Hence, the OMR is a kind of holonomic robot [2]. Because of its Euler-Lagrange dynamics, the recognized "classical" control techniques for robot manipulators [3] have been adapted for controlling this kind of mobile robot. Recently, intensive and notable research has been devoted to this device (see, e.g., [1, 4–6] and references therein).

To implement the control strategies, a localization system is required to estimate the actual wheeled mobile robot positions and velocities [7], which are mainly based on the odometric data, the robot kinematics, and the Kalman filter. Nevertheless, since there exists a maximum sampling time to reconstruct the velocity of the wheels, the odometric data could have errors if the Nyquist-Shannon criteria are not satisfied. Hence, the important issue to consider during the control design is the inclusion of the physical limitations of the system, such as bounds in velocities and/or torques. For instance, high velocities developed by the mobile robot can result in a higher probability of wheel slides and deviations from the desired trajectory. In practice, the mobile robot has bounded velocities and torques which should never

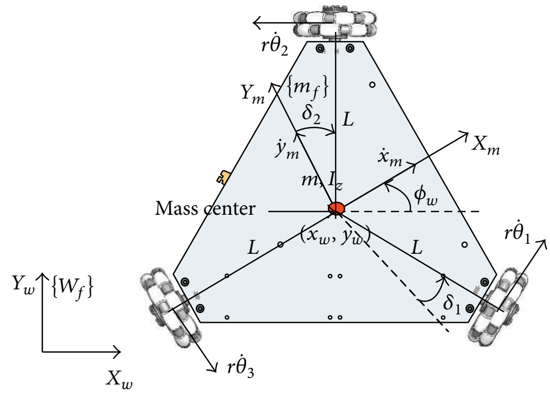

Figure 1: Diagram of the holonomic omnidirectional mobile robot.

be exceeded. If the control strategy is designed without considering these constraints, the system could exhibit poor performance and even instability [8].

Many control strategies in robotics have been proposed without considering explicitly the physical limits of the system. One of the underlying assumptions is that the robot task can be smoothly tailored in space and scaled in time so as to fit to the system limitations. However, simply scaling of the task commands could recover motion feasibility but may no longer satisfy the tracking performance [9]. The above description requires off-line planning of the desired trajectory. This may result to be impractical in some applications, for example, when the desired trajectory is available while the robot is in motion or under unpredictable situations in human-robot interaction systems, in which the speed and acceleration magnitude become high during a short time interval. Online trajectory scaling schemes have been proposed in [10–13], mainly to satisfy torque limits. Moreover, simple hardware and/or software saturation of the commands results in the lack of execution of the desired motion [14].

Control of robots with bounded velocities and torques has proved to be challenging problems, and these have been addressed mainly for robot manipulators. For instance, on one hand, interesting contributions for robot manipulators with bounded torques are reported in [8–17]. On the other hand, control of robot manipulators with bounded velocities is considered in [18–25]. Control of mobile robots with bounded torques is reported in [26] and that with velocity constraints is reported in [27–31]. However, among all these results, a common characteristic is that the considered system is subject to different operation conditions, and its performance is deteriorated when the signals are saturated. Also, some of them do not completely guarantee the given limits during the system transitory stage, even when the initial conditions of the states are within the specified bounds. A formal stability analysis is missed in many of these works, and with few exceptions, the results are mainly valid for set-point regulation or for the case in which the kinematic model of the system is considered.

In this paper, we focus our attention on the motion control problem of the OMR subject to velocity constraints. Different from that reported in [27–31], the solution proposed here consists in the redesign of a well-known tracking controller to achieve global asymptotic tracking with desired bounded velocities, considering the dynamic model of the system. The proposed control scheme includes explicitly the desired bounds for the developed Cartesian velocities, which in turn bound the maximal velocities developed by the wheels. These bounds are freely set by the user considering the physical limits of the device. The proposal includes a tracking controller (TC) combined with a passive nonlinear controller (PNC) through a negative feedback connection structure. The TC is used to achieve the desired tracking performance, while the PNC is used to ensure bounded velocities. By using Lyapunov theory and passivity tools, global asymptotic tracking with desired bounded velocities is proved. Simulations and experimental results are provided to show the effectiveness of the proposed control strategy.

The rest of the paper is organized as follows. In Section 2, the dynamics of the considered mobile robot is given, and the problem formulation is stated. The main result of the proposed control system, and its stability analysis, is presented in Section 3. Simulations and real-time experiments are given in Section 4. Finally, some conclusions and future work ideas are given in Section 5.

2. Problem Formulation

2.1. Dynamic Model. Consider the OMR shown in Figure 1, whose dynamics is described by

$$\Sigma: M(q)\ddot{q} + C(q,\dot{q})\dot{q} = B(q)\tau, \tag{1}$$

where $q = [x_w, y_w, \phi_w]^\top$ is the configuration vector, which includes linear and angular positions of the center of mass of the OMR with respect to the inertial frame (X_w, Y_w), $\dot{q}$ is the velocity vector, $\ddot{q}$ is the acceleration vector, and $\tau \in \mathbb{R}^3$ is the control input which includes the torques applied to the wheels. $M(q) \in \mathbb{R}^{3\times3}$ is the inertia matrix, $C(q,\dot{q})\dot{q} \in \mathbb{R}^3$ is the Coriolis and centrifugal force vector, and $B(q) \in \mathbb{R}^{3\times3}$ is the input matrix. These are given as

$$M(q) = \begin{bmatrix} m + \dfrac{3J}{2r^2} & 0 & 0 \\ 0 & m + \dfrac{3J}{2r^2} & 0 \\ 0 & 0 & I_z + \dfrac{3JL^2}{r^2} \end{bmatrix},$$

$$C(q,\dot{q}) = \begin{bmatrix} 0 & \dfrac{3J}{2r^2}\dot{\phi}_w & 0 \\ -\dfrac{3J}{2r^2}\dot{\phi}_w & 0 & 0 \\ 0 & 0 & 0 \end{bmatrix}, \quad (2)$$

$$B = \begin{bmatrix} -\dfrac{1}{2r}\left(\sin(\phi_w) - \sqrt{3}\cos(\phi_w)\right) & \dfrac{1}{r}\sin(\phi_w) & -\dfrac{1}{2r}\left(\sin(\phi_w) + \sqrt{3}\cos(\phi_w)\right) \\ \dfrac{1}{2r}\left(\cos(\phi_w) + \sqrt{3}\sin(\phi_w)\right) & -\dfrac{1}{r}\cos(\phi_w) & \dfrac{1}{2r}\left(\cos(\phi_w) - \sqrt{3}\sin(\phi_w)\right) \\ \dfrac{L}{r} & \dfrac{L}{r} & \dfrac{L}{r} \end{bmatrix}.$$

The system parameters correspond to those of a physical prototype and are listed in Table 1. The dynamics of the OMR has the following properties [1].

(**P1**) The inertia matrix $M(q)$ and its inverse are symmetric and positive definite for all q. The inverse of the inertia matrix is bounded for all q by a positive constant μ as $\|(M(q))^{-1}\| \le \mu$.

(**P2**) The Coriolis and centrifugal force vector $C(q,\dot{q})\dot{q}$ satisfies $\|C(q,\dot{q})\dot{q}\| \le \alpha\|\dot{q}\|^2$, for all q, $\dot{q}$, and some positive constant α.

(**P3**) The input matrix $B(q)$ is positive definite for all q. Its inverse is denoted by $\overline{B}(q) = (B(q))^{-1}$.

2.2. Problem Statement. Suppose that there exists a controller τ_C which makes the system Σ to asymptotically track a desired trajectory $q_d(t)$ (i.e., by choosing for (1) the input $\tau = \tau_C$, the closed-loop system dynamics behaves such that $\lim_{t\to\infty} q(t) = q_d(t)$). However, τ_C has been designed without considering the velocity constraints in the system. So, we are interested in redesigning the given tracking controller to achieve asymptotic tracking with desired bounded velocities.

For $i \in \{1,2,3\}$, let $\dot{q}_i$ denote the ith velocity of the system Σ. Also, let the negative and positive constants $\bar{\dot{q}}_{i_L}$ and $\bar{\dot{q}}_{i_U}$ denote the desired lower and upper bounds, respectively, for the ith velocity. These bounds are freely set by the user considering the physical capabilities of the system. Define the following complementary sets:

$$\mathcal{I}_i = \left\{\dot{q}_i \mid \dot{q}_i \in \left[\bar{\dot{q}}_{i_L}, \bar{\dot{q}}_{i_U}\right]\right\},$$
$$\mathcal{O}_i = \left\{\dot{q}_i \mid \dot{q}_i \in \left\{\mathbb{R} \setminus \mathcal{I}_i\right\}\right\}. \quad (3)$$

Then, it is said that $\dot{q}_i$ is within specifications, if and only if $\dot{q}_i \in \mathcal{I}_i$, while it is out of specifications if and only if $\dot{q}_i \in \mathcal{O}_i$.

Therefore, the controller redesign to be developed must be capable of achieving asymptotic tracking with desired bounded velocities, either $\dot{q}_i \in \mathcal{I}_i$ or $\dot{q}_i \in \mathcal{O}_i$. More precisely, the following objectives must be achieved:

$$\lim_{t\to\infty}\left[q_i(t) - q_{d_i}(t)\right] = 0, \quad (4)$$

$$\lim_{t\to\infty}\left[\dot{q}_i(t) - \dot{q}_{d_i}(t)\right] = 0, \quad (5)$$

$$\bar{\dot{q}}_{i_L} \le \dot{q}_i(t) \le \bar{\dot{q}}_{i_U} \quad \forall t \ge T, \quad (6)$$

for $i \in \{1,2,3\}$ and some finite time $T \ge 0$.

Throughout the paper, it is assumed that all variables in the system are measurable, and its parameters are known.

3. Control Design

3.1. Tracking Controller. Given the desired vector of reference $q_d(t)$, define the tracking errors:

$$\tilde{q} = q - q_d, \qquad \dot{\tilde{q}} = \dot{q} - \dot{q}_d, \qquad \ddot{\tilde{q}} = \ddot{q} - \ddot{q}_d, \quad (7)$$

and consider for the system Σ the "classical" computed torque controller [1, 3]:

$$\tau_{CT} = \overline{B}(q)\left[M(q)\left[\ddot{q}_d - K_D\dot{\tilde{q}} - K_P\tilde{q}\right] + C(q,\dot{q})\dot{q}\right], \quad (8)$$

where K_P, K_D are constant positive definite diagonal matrices, which are chosen accordingly to the desired tracking

Table 1: Parameters of the omnidirectional mobile robot.

Parameter	Description	Value	Units
δ_1	Angle for position of wheel 1	$\pi/6$	rad
δ_2	Angle for position of wheel 2	$\pi/3$	rad
J	Wheel's inertia	$5.82E-4$	kg·m^2
I_z	Mobile's inertia	0.0127	kg·m^2
m	Mass	11.83	kg
r	Wheel's radius	0.0625	m
L	Distance to the wheels	0.287	m

performance (see, e.g., [3]). It is well known that the closed-loop dynamics, obtained by placing (8) in (1) with $\tau = \tau_{\text{CT}}$, is described by the decoupled second-order linear system:

$$\ddot{\tilde{q}} + k_D\dot{\tilde{q}} + k_P\tilde{q} = 0, \tag{9}$$

whose stability properties are set through the control gains k_P and k_D. This tracking controller allows Σ to achieve asymptotic tracking (4)-(5), but not with bounded velocities (6).

3.2. Tracking Controller with Desired Bounded Velocities

3.2.1. A Static Nonlinear Function. Let $F : \mathbb{R}^3 \mapsto \mathbb{R}^3$ be a continuous nonlinear vector function of the form

$$F(\dot{q}) = \begin{bmatrix} f_1(\dot{q}_1) \\ f_2(\dot{q}_2) \\ f_3(\dot{q}_3) \end{bmatrix}, \tag{10}$$

whose elements, denoted by $f_i(\dot{q}_i)$, are defined as follows:

$$f_i(\dot{q}_i) = \begin{cases} 1, & \dot{q}_i < \bar{\dot{q}}_{i_L}, \\ \dfrac{1-\cos\left((\pi/\Delta_i)\left(\dot{q}_i + \bar{\dot{q}}_{i_L} - \Delta_i\right)\right)}{2}, & \\ & \bar{\dot{q}}_{i_L} \le \dot{q}_i < \bar{\dot{q}}_{i_L} + \Delta_i, \\ 0, & \bar{\dot{q}}_{i_L} + \Delta_i \le \dot{q}_i \le \bar{\dot{q}}_{i_U} - \Delta_i, \\ \dfrac{-1+\cos\left((\pi/\Delta_i)\left(\dot{q}_i - \bar{\dot{q}}_{i_U} + \Delta_i\right)\right)}{2}, & \\ & \bar{\dot{q}}_{i_U} - \Delta_i < \dot{q}_i \le \bar{\dot{q}}_{i_U}, \\ -1, & \dot{q}_i > \bar{\dot{q}}_{i_U}, \end{cases} \tag{11}$$

for $i \in \{1,2,3\}$. Note that the proposed function is a combination of a dead zone and a saturation, with a smooth transition interval defined by the small positive constant Δ_i. Figure 2 shows the shape of $f_i(\dot{q}_i)$.

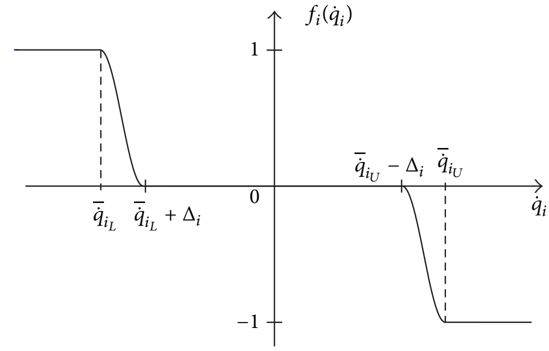

Figure 2: Shape of the proposed function $f_i(\dot{q}_i)$.

Let A be a positive definite diagonal matrix. Its elements, denoted by a_i, are constant or possibly time-varying. In either case, they are strictly positive for all time; that is,

$$A = \operatorname{diag}\{a_i\} > 0 \quad \forall t, i \in \{1,2,3\}. \tag{12}$$

The entries a_i are yet to be defined.

Proposition 1. *Let A be the diagonal matrix (12) and let $F(\dot{q})$ be the nonlinear function defined in (10)-(11). Then, the product $-\dot{q}^\top AF(\dot{q})$ is passive.*

Proof. By definition of $f_i(\dot{q}_i)$, the product $\dot{q}_i f_i(\dot{q}_i)$ is negative semidefinite for all $\dot{q}_i$, and A is positive definite (12), so

$$-\dot{q}AF(\dot{q}) = -\sum_{i=1}^{3}\dot{q}_i a_i f_i(\dot{q}_i) \ge 0, \quad \forall t, \dot{q}. \tag{13}$$

Since the product is positive semidefinite, it is passive. □

Proposition 2. *Consider the velocity error $\dot{\tilde{q}}$ defined in (7), the diagonal matrix A given in (12), and the nonlinear function $F(\dot{q})$ defined in (10)-(11). Then, the product $-\dot{\tilde{q}}^\top AF(\dot{q})$ is passive if the desired velocity bounds are set freely by the user taking into account the relation:*

$$\bar{\dot{q}}_{i_L} + \Delta_i \le \dot{q}_{d_i}(t) \le \bar{\dot{q}}_{i_U} - \Delta_i, \quad \forall t, i \in \{1,2,3\}. \tag{14}$$

Proof. Let us write the product $-\dot{\tilde{q}}^\top AF(\dot{q})$ in the form

$$-\dot{\tilde{q}}^\top AF(\dot{q}) = \sum_{i=1}^{3}\left(\dot{q}_{d_i} - \dot{q}_i\right) a_i f_i(\dot{q}_i). \tag{15}$$

Then the following cases are analysed.

(i) If $\dot{q}_i \in \mathcal{F}_i$, and if $\dot{q}_i \in [\bar{\dot{q}}_{i_L} + \Delta_i, \bar{\dot{q}}_{i_U} - \Delta_i]$, then $f_i(\dot{q}_i) = 0$ (see (11) and Figure 2), and therefore the ith element of (15) is zero; that is,

$$\left(\dot{q}_{d_i} - \dot{q}_i\right) a_i f_i(\dot{q}_i) = 0. \tag{16}$$

TABLE 2: Positivity of the ith element of (15).

$\dot{q}_i$	$\dot{q}_{di}$	$(\dot{q}_{di} - \dot{q}_i)$	$f_i(\dot{q}_i)$	$(\dot{q}_{di} - \dot{q}_i)a_i f_i(\dot{q}_i)$
−	−	+	+	+
−	+	+	+	+
+	−	−	−	+
+	+	−	−	+

(ii) If $\dot{q}_i \in \mathcal{I}_i$, and more precisely, if either $\dot{q}_i \in [\overline{\dot{q}}_{i_L}, \overline{\dot{q}}_{i_L} + \Delta_i)$ or $\dot{q}_i \in (\overline{\dot{q}}_{i_U} - \Delta_i, \overline{\dot{q}}_{i_U}]$, it is clear that $|\dot{q}_{d_i}| < |\dot{q}_i|$ from (14). Then, with aid of Table 2, it is concluded that the ith element of (15) is positive definite; that is,

$$\left(\dot{q}_{d_i} - \dot{q}_i\right) a_i f_i\left(\dot{q}_i\right) > 0. \tag{17}$$

(iii) If $\dot{q}_i \in \mathcal{O}_i$, then $|\dot{q}_{d_i}| < |\dot{q}_i|$, and obviously $|\dot{q}_i| \neq 0$. As in the previous case, Table 2 helps us to conclude that the ith element of (15) is positive definite; that is, (17) is satisfied again.

From the previous analysis, one has that (15) is either zero or positive definite for all $\dot{q}_i$. Then,

$$-\dot{\tilde{q}}^{\top} AF\left(\dot{q}\right) = \sum_{i=1}^{3}\left(\dot{q}_{d_i} - \dot{q}_i\right) a_i f_i\left(\dot{q}_i\right) \geq 0 \quad \forall t, \dot{\tilde{q}}, \dot{q}. \tag{18}$$

Since the product is positive semidefinite, it is passive. □

3.2.2. Control Redesign. Now, to bound the velocities of the OMR, the following nonlinear controller is proposed:

$$\tau_{\mathrm{LV}} = \overline{B}\left(q\right) M\left(q\right) AF\left(\dot{q}\right), \tag{19}$$

where the elements of the diagonal matrix A are defined as

$$a_i = \lambda_i + \left\|z_i\right\|, \tag{20}$$

where λ_i is a positive constant, and

$$z_i = \ddot{q}_d - k_{D_i}\dot{\tilde{q}}_i - k_{P_i}\tilde{q}_i. \tag{21}$$

Note that (12) is satisfied with this definition of a_i.

To achieve asymptotic tracking with desired bounded velocities, the foregoing controller must be used simultaneously with the tracking controller. To this aim, the following bounded-velocity controller for trajectory tracking is finally proposed for the system Σ:

$$\begin{aligned}\tau_{\mathrm{BV}} = {} & \underbrace{\overline{B}\left(q\right)\left[M\left(q\right)\left[\ddot{q}_d - k_D\dot{\tilde{q}} - k_P\tilde{q}\right] + C\left(q,\dot{q}\right)\dot{q}\right]}_{\tau_{\mathrm{CT}}} \\ & + \underbrace{\overline{B}(q)M(q)AF(\dot{q})}_{\tau_{\mathrm{LV}}},\end{aligned} \tag{22}$$

where τ_{CT} is exactly the computed torque controller given in (8), used to asymptotically track the desired reference, while τ_{LV} is the nonlinear controller (19), used to keep the velocities within its limits.

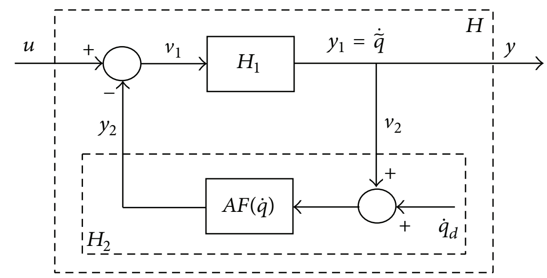

FIGURE 3: Negative feedback connection H_1-H_2.

Theorem 3. *Given the OMR dynamics (1), together with its properties, and a smooth desired reference $\dot{q}_d(t)$ to be tracked, consider desired bounds for the velocities to be developed by the mobile robot which are freely set considering (14). Then, taking for Σ the control input $\tau = \tau_{BV}$, where τ_{BV} is given in (22), global asymptotic tracking with bounded velocities is achieved.*

Proof. Take for Σ the control input $\tau = \tau_{\mathrm{BV}}$ (i.e., place (22) in (1)) to obtain the closed-loop dynamics:

$$\ddot{\tilde{q}} + k_D\dot{\tilde{q}} + k_P\tilde{q} - AF\left(\dot{q}\right) = 0, \tag{23}$$

which represents the system H, shown in Figure 3, consisting of the negative feedback connection of H_1 and H_2. These systems are described by

$$\begin{aligned} H_1&: \begin{cases}\ddot{\tilde{q}} + k_D\dot{\tilde{q}} + k_P\tilde{q} = v_1, \\ y_1 = \dot{\tilde{q}},\end{cases} \\ H_2&: \left\{\, y_2 = -AF\left(\dot{q}\right) = -AF\left(v_2 + \dot{q}_d\right) = -AF\left(\dot{\tilde{q}} + \dot{q}_d\right),\right.\end{aligned} \tag{24}$$

with the connections

$$\begin{aligned} v_1 &= u - y_2, \\ v_2 &= y_1,\end{aligned} \tag{25}$$

where $u \equiv 0$. Note that H_1 corresponds to (9).

Hereafter, the proof is presented in two steps. First, global asymptotic tracking is proved by showing that the system H is output strictly passive and zero-state observable (see, e.g., [32, 33] for definitions, properties, and results of dissipative systems). Second, bounded velocities are proved by showing that the set $\mathcal{I}_i$ is attractive.

Passivity. We start by proving that both systems H_1 and H_2 are passive.

(i) First, consider the system H_1 of the feedback connection shown in Figure 3 and described in (24). Take the time derivative of the (radially unbounded) positive definite storage function:

$$S\left(\tilde{q}, \dot{\tilde{q}}\right) = \frac{1}{2}\tilde{q}^{\top}k_P\tilde{q} + \frac{1}{2}\dot{\tilde{q}}^{\top}\dot{\tilde{q}}, \tag{26}$$

along H_1 to obtain

$$\dot{S}\left(\tilde{q}, \dot{\tilde{q}}\right) = \dot{\tilde{q}}^{\top}v_1 - \dot{\tilde{q}}^{\top}k_D\dot{\tilde{q}} = y_1^{\top}v_1 - y_1^{\top}k_D y_1. \tag{27}$$

The foregoing equation clearly states that H_1 is output strictly passive. Moreover, H_1 is zero-state observable (see Definition 6.5 in [32]), since $\tilde{q} = 0$ is the unique solution which can stay in the set

$$\mathcal{Z}_1 = \{\tilde{q} \in \mathbb{R}^n \mid y_1 = 0,\ v_1 = 0\} = \{k_P\tilde{q} = 0\}, \tag{28}$$

for k_P positive definite.

(ii) Second, for the static nonlinear function described by H_2 in (24), and connected to H_1 by the negative feedback connection shown in Figure 3, its input-output product is

$$y_2^\top v_2 = v_2^\top y_2 = \dot{\tilde{q}}^\top \left(-AF\left(\dot{\tilde{q}} + \dot{q}_d\right)\right) = -\dot{\tilde{q}}^\top AF\left(\dot{q}\right). \tag{29}$$

From Proposition 2, it is clear that H_2 is passive.

Then, since H_1 and H_2 are both passive systems, the whole negative feedback connection H is passive (Theorem 6.1 in [32]). Note that the storage function (26) is still valid for system H with the connections (25). The time derivative of the storage is

$$\begin{aligned}\dot{S} &= y_1^\top u - y_1^\top k_D y_1 - y_1^\top y_2 = y^\top u - y^\top k_D y - \underbrace{\left(-\dot{\tilde{q}}^\top AF\left(\dot{q}\right)\right)}_{\geq 0} \\ &\leq y^\top u - y^\top k_D y,\end{aligned} \tag{30}$$

so H is output strictly passive.

Global Asymptotic Tracking. For system H, take $y = 0$ and $u = 0$ to obtain the set $\mathcal{Z} = \{k_P\tilde{q} = 0\}$ (note that $y = \dot{\tilde{q}} = 0$ implies that $\dot{q}_d \equiv \dot{q}$, and using (14), one obtains $|\dot{q}_i| < \bar{\dot{q}}_i$, so $F(\dot{q}) \equiv 0$, and therefore $-A(t)F(\dot{q}) \equiv 0$ in (23)). Since $\tilde{q} = 0$ is the unique solution which can stay in $\mathcal{Z}$, the system H is zero-state observable. Now, following Lemma 6.7 in [32], since H is output strictly passive and zero-state observable, it is concluded that $\tilde{q} = 0$ is globally asymptotically stable (the storage function (26) is radially unbounded). This finally proves (4)-(5).

Bounded Velocities. Considering (23), the system is under the action of the proposed controller. Then, if $\dot{q}_i \in \mathcal{I}_i$ with $\dot{q}_i \in [\bar{\dot{q}}_{i_L} + \Delta_i, \bar{\dot{q}}_{i_U} - \Delta_i]$, one has that $f_i(\dot{q}_i) = 0$, which implies that $\tau_{\text{LV}} = 0$, and $\dot{q}_i$ is driven only with the tracking controller (i.e., $\tau = \tau_{\text{CT}}$). As a consequence, asymptotic tracking of the reference will be achieved, as it was already proved, and the velocities are bounded. However, the tracking controller could make $\dot{q}_i$ increase rapidly its speed towards the desired bound $\bar{\dot{q}}_i$. But inasmuch as $\dot{q}_i$ approaches the bounds, the magnitude of τ_{LV} also increases rapidly in accordance with $f_i(\dot{q}_i)$, causing $\dot{q}_i$ not to leave the set $\mathcal{I}_i$. In case that $\dot{q}_i \in \mathcal{O}_i$, one has that $\dot{q}_i$ is driven fastly, in finite time, to the set $\mathcal{I}_i$.

The above description corresponds to the attractive behaviour of $\mathcal{I}_i$, which is ensured from (23), and it is now proved. To this aim, define

$$\begin{aligned}\bar{\dot{q}}_i &= \min\left(\left|\bar{\dot{q}}_{i_L}\right|, \bar{\dot{q}}_{i_U}\right), \\ \sigma_i &= \frac{1}{2}\left(\dot{q}_i^2 - \bar{\dot{q}}_i^2\right) > 0 \quad \forall \dot{q}_i \in \mathcal{O}_i.\end{aligned} \tag{31}$$

Note that $\sigma_i = 0$ implies that $\dot{q}_i \in \mathcal{I}_i$. The dynamics of σ_i is thus described by

$$\dot{\sigma}_i = \dot{q}_i\ddot{q}_i. \tag{32}$$

Take the time derivative of

$$V_i\left(\sigma_i\right) = \frac{1}{2}\sigma_i^2, \tag{33}$$

along (32) to obtain

$$\dot{V}_i\left(\sigma_i\right) = \sigma_i\dot{\sigma}_i = \sigma_i\dot{q}_i\ddot{q}_i. \tag{34}$$

By definition, σ_i is positive definite, so we focus on the analysis of the product $\dot{q}_i\ddot{q}_i$.

Considering (7) and (21), the closed-loop dynamics (23) can be written in the form

$$\ddot{q} = z_i + a_i f_i\left(\dot{q}_i\right), \tag{35}$$

and then the product $\dot{q}_i\ddot{q}_i$ is written as

$$\dot{q}_i\ddot{q}_i = \dot{q}_i\left(z_i + a_i f_i\left(\dot{q}_i\right)\right) \leq \left|\dot{q}_i\right| \cdot \left|z_i\right| + \dot{q}_i a_i f_i\left(\dot{q}_i\right). \tag{36}$$

Since $\dot{q}_i \in \mathcal{O}_i$, it is true that

$$\dot{q}_i a_i f_i\left(\dot{q}_i\right) = -a_i\left|\dot{q}_i\right|, \tag{37}$$

and using (20), one has that

$$\left|\dot{q}_i\right| \cdot \left|\dot{z}_i\right| + \dot{q}_i a_i f_i\left(\dot{q}_i\right) \leq \left|\dot{q}_i\right| \cdot \left|\dot{z}_i\right| - a_i\left|\dot{q}_i\right| \leq -\lambda\left|\dot{q}_i\right|. \tag{38}$$

Therefore,

$$\dot{q}_i\ddot{q}_i \leq -\lambda\left|\dot{q}_i\right| < 0, \tag{39}$$

and going back to (34), one finally has

$$\sigma_i\dot{\sigma}_i \leq -\lambda\left|\sigma_i\right|\left|\dot{q}_i\right| < 0, \tag{40}$$

which states that $\sigma_i = 0$ is reached in finite time (see, e.g., [34]). Moreover, (39) states that the ith velocity and acceleration have opposite signs, which proves that $\dot{q}_i$ will not leave $\mathcal{I}_i$. Therefore, $\mathcal{I}_i$ is attractive, and the velocities will remain bounded, satisfying (6). □

4. Simulations and Real-Time Experiments

The aim of this section is to illustrate the effectiveness of the proposed control scheme (22) via numerical simulations and real-time experiments. These consist in the tracking control of an OMR with desired bounded velocities. With the purpose to include a reference to better illustrate the capabilities

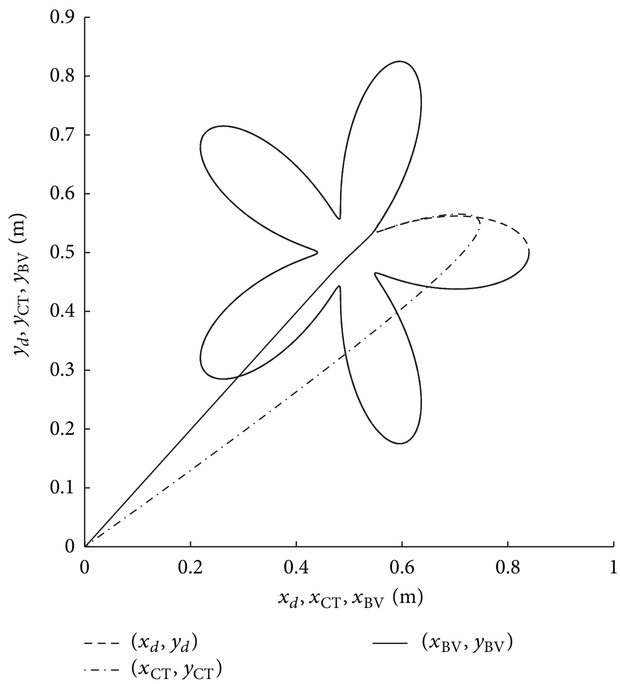

FIGURE 4: Simulation results of the task space trajectories described by the OMR under the action of the CT and BV controllers.

of the proposal (22), the simulations and experiments are also developed for the OMR with the computed-torque controller (8), which allows the system to be controlled without bounding its velocities.

Consider the OMR described in Section 2.1, and let the desired smooth trajectory be a "Daisy," whose parametric equations are [6]

$$x_d(t) = \frac{1}{2} + b_t\left(a_t + r_t\cos(m\omega t)\right)\cos(\omega t),$$
$$y_d(t) = \frac{1}{2} + b_t\left(a_t + r_t\cos(m\omega t)\right)\sin(\omega t), \tag{41}$$
$$\phi_d(t) = \cos(\omega t).$$

The trajectory has an external radius of $b_t(a_t + r_t)$ and is centred at the point (in the Cartesian space) $x = 0.5$ [m] and $y = 0.5$ [m]. The values of its parameters are $a_t = 1$ [m], $r_t = 0.7$ [m], $b_t = 0.2$ (a scaling factor adjusting the trajectory to the working area), and $m = 5$ (the number of petals). Also, $\omega = 2\pi/25$ leads the OMR to track a whole turn in 25 s.

Considering this trajectory, the desired velocity bounds are set as follows: $\overline{\dot{x}}_L = -0.2$ [m/s], $\overline{\dot{x}}_U = 0.25$ [m/s], $\overline{\dot{y}}_L = -0.2$ [m/s], $\overline{\dot{y}}_U = 0.25$ [m/s], $\overline{\dot{\phi}}_L = -0.35$ [rad/s], and $\overline{\dot{\phi}}_U = 0.3$ [rad/s]. Also, the parameters for the proposed BV controller are set as $\Delta_i = 0.0125$ and $\lambda_i = 1$, for $i \in \{1, 2, 3\}$.

In all the graphics to be presented, to distinguish the system performance under the action of the different controllers, the following subscripts are used in the signals: CT for the computed-torque controller (8), and BV for the proposed bounded-velocity trajectory tracking controller (22)

4.1. Simulations. Simulations were developed in MATLAB/Simulink with a fixed-step Euler method at 1 ms. The initial condition of the OMR was $q(0) = \begin{bmatrix}0 & 0 & 0 & 0 & 0 & 0\end{bmatrix}^\top$, and the desired tracking performance was specified, following [3], through $K_P = \mathrm{diag}\{\omega_n^2\}$, and $K_D = \mathrm{diag}\{2\xi\omega_n\}$, where $\xi = 0.85$ is the desired damping ratio and $\omega_n = 5$ [rad/s] is the desired undamped natural frequency.

Figures 4 to 7 show the system behaviour under the action of the CT and BV controllers. For the CT controller, asymptotic tracking is completely achieved in approximately 2.5 s (see Figures 5 and 6, dashed-dot lines), and note that the system develops maximal velocities of about 1.5 rad/s (see Figure 6, dashed-dot lines). Then, for the OMR under the CT controller, it is clear that the desired velocity constraints (dotted lines) are not satisfied with the given tracking performance. However, with the proposed redesign (22), the BV controller, both asymptotic tracking and desired bounded velocities are completely achieved (see Figures 5 and 6, solid lines). This is achieved at the cost of greater convergence times, which is natural as the velocities do remain constrained to the desired maximal values. During the transitory stage, note that the velocity tracking errors are reduced as the velocities remain bounded (with the BV controller, the system velocities are kept closer to the desired velocities to be tracked). Also, as shown in Figure 7, a benefit of having bounded velocities is to require reduced control efforts (because the proposed BV controller dissipates the excess of energy in the system when the velocities remain bounded).

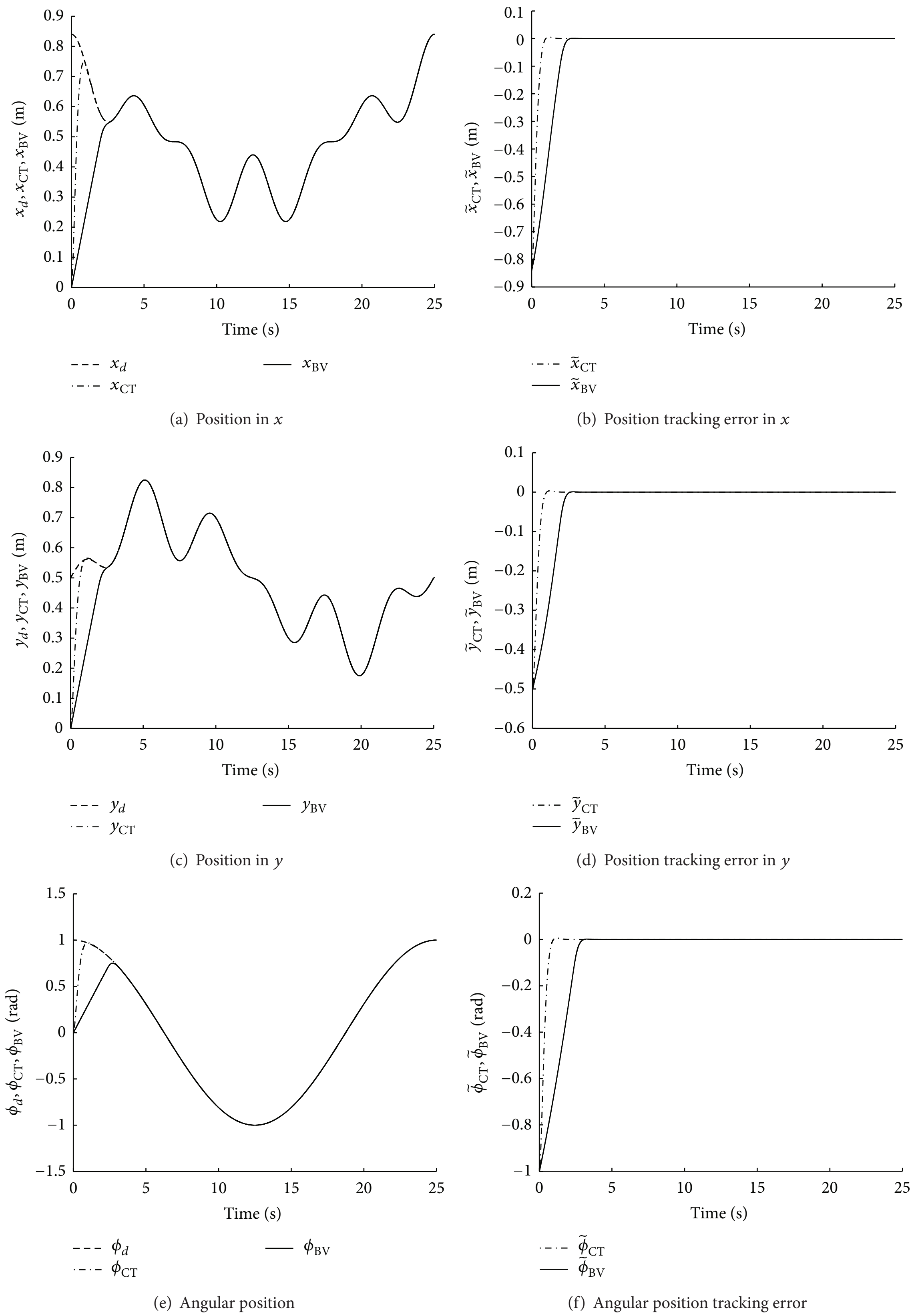

FIGURE 5: Simulation results of the positions and tracking errors of the OMR under the action of the CT and BV controllers.

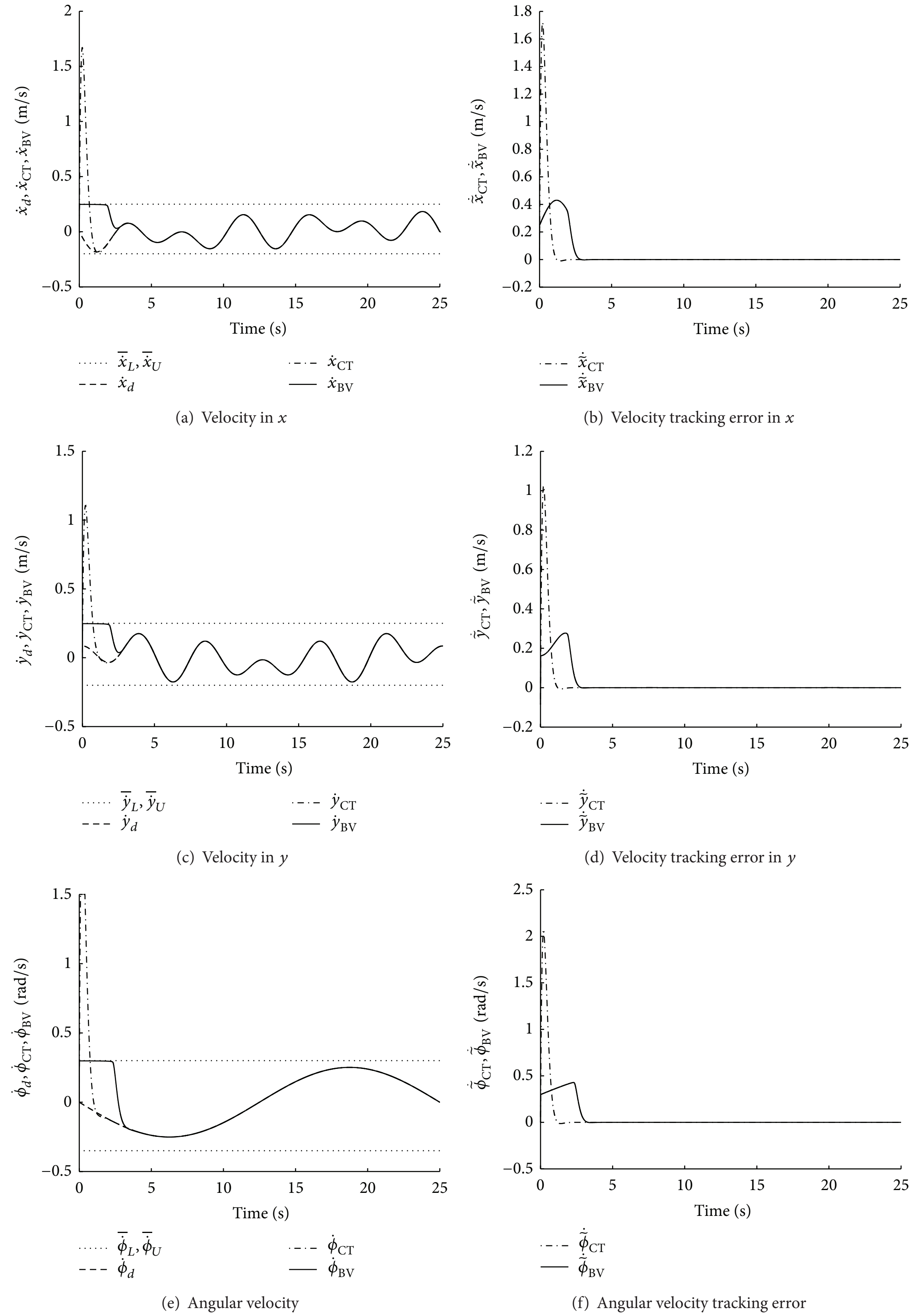

(a) Velocity in x

(b) Velocity tracking error in x

(c) Velocity in y

(d) Velocity tracking error in y

(e) Angular velocity

(f) Angular velocity tracking error

Figure 6: Simulation results of the velocities and tracking errors of the OMR under the action of the CT and BV controllers.

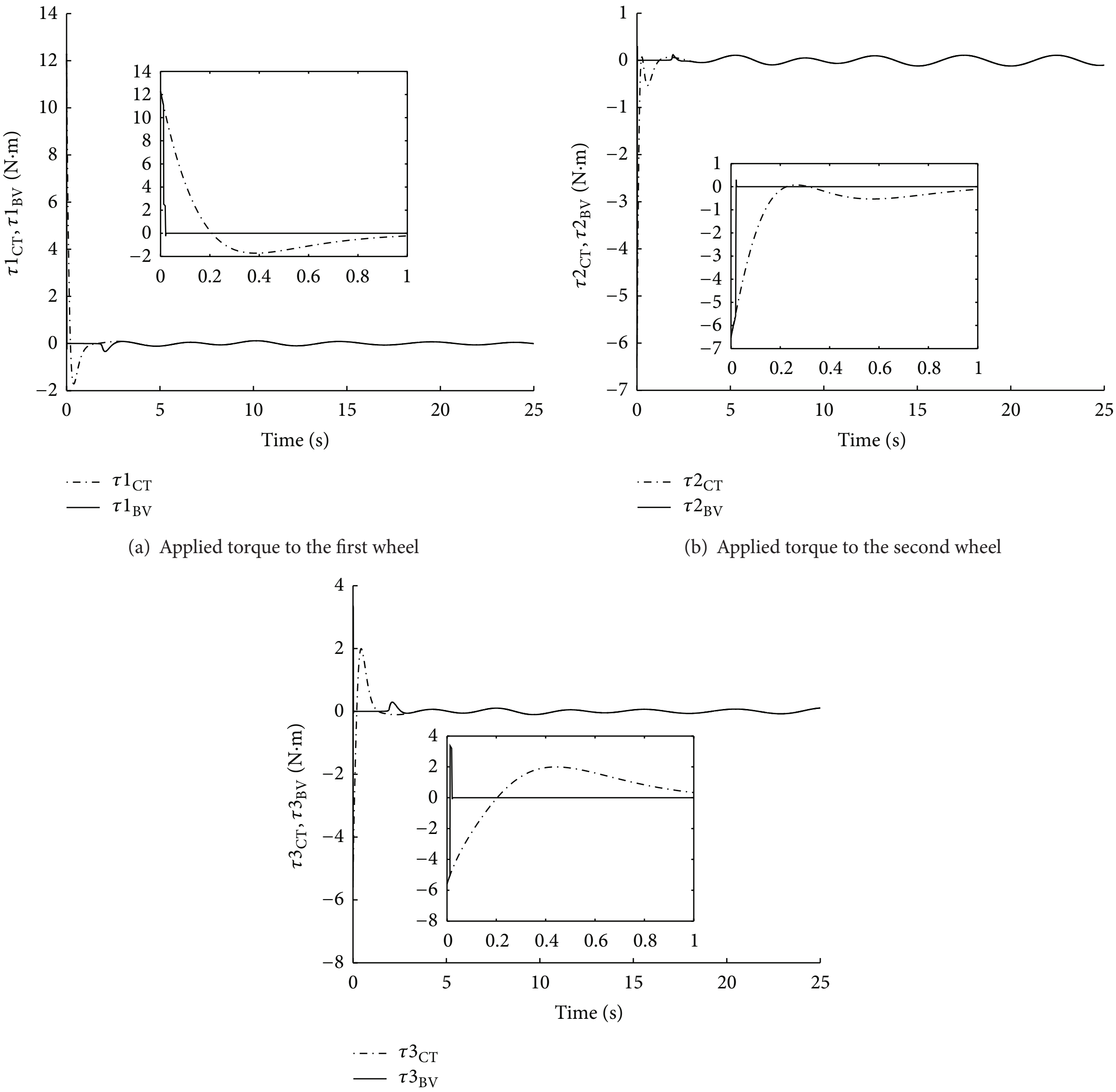

(a) Applied torque to the first wheel

(b) Applied torque to the second wheel

(c) Applied torque to the third wheel

FIGURE 7: Simulation results of the torques applied to the OMR under the action of the CT and BV controllers.

4.2. Real-Time Experiments. Real-time experiments were carried out in the mobile robot prototype shown in Figure 8, which has been designed to maximize its dexterity (see [35]). The dynamics of the system, as well as its parameters, correspond to those given in Section 2.1.

Considering the CT controller, the desired tracking performance was specified, following [3], through the control parameters $k_{P_i} = \omega_{n_i}^2$ and $k_{D_i} = 2\xi_i\omega_{n_i i}$, for $i \in \{1, 2, 3\}$. These were set to $\omega_{n1} = \omega_{n2} = 23.45$, $\omega_{n3} = 31.62$ [rad/s], $\xi_1 = \xi_2 = 1.067$, and $\xi_3 = 0.79$. Also, for the BV controller, we have taken $\Delta_i = 0.01$, and $\lambda_i = 0.1$.

Figures 9 to 12 show the real-time system behaviour under the action of the CT and BV controllers. It can be seen in Figure 11 that the CT controller alone does not allow the system to satisfy the desired velocity bounds. This is not the case for the BV controller, which in fact behaves similar to the CT controller when all the velocities are within their limits, but away of the bounds (see Figures 11 and 12). Note that, for both controllers, convergence to the reference trajectory is achieved at almost the same instant of time, but with bounded errors (see Figures 10 and 11). Among other reasons, these errors could have been produced by the inaccuracy of the dynamic model used to derive the control scheme. The experimental results are very similar to those obtained by numerical simulations and are consistent to the theoretical development.

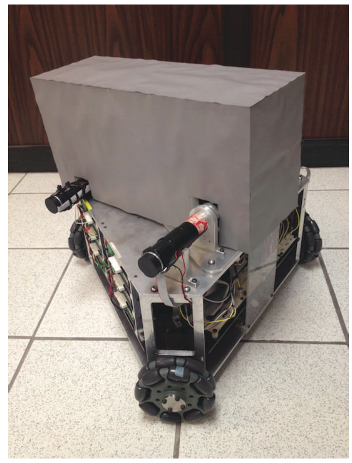

Figure 8: Physical prototype of the omnidirectional mobile robot.

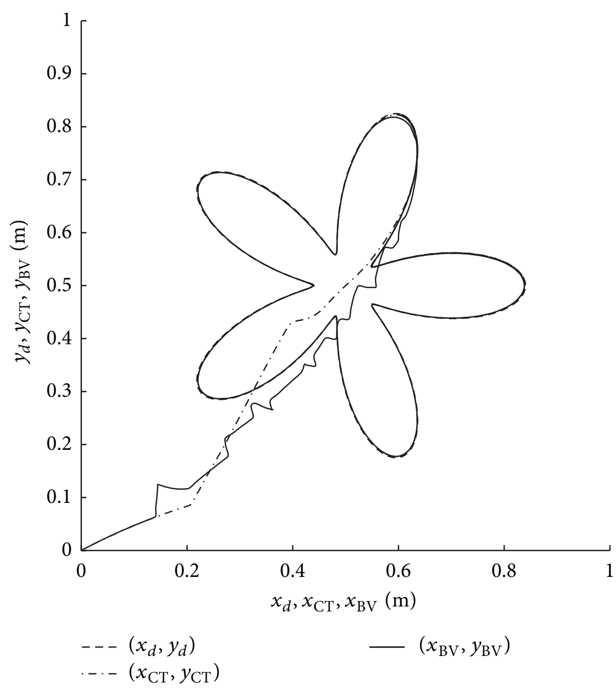

Figure 9: Experimental results of the task space trajectories described by the OMR under the action of the CT and BV controllers.

5. Conclusions and Future Work

A solution to achieve global asymptotic tracking with desired bounded velocities for an omnidirectional mobile robot was proposed. It consisted in the redesign of a tracking controller to take into account, explicitly, the velocity constraints of the system. The stability analysis was developed using Lyapunov and passivity tools. Simulation and experimental results showed the effectiveness of the proposal.

The ideas proposed here can be extended to use other tracking controllers to further improve the system performance. This can be done immediately with those allowing the preservation of the passivity properties of the closed-loop system. Also, the extension can be done to bound other important variables in the system, like positions, accelerations, and torques. Among others, applications of these ideas in parallel robotics, aerial vehicles, and human-robot interaction are visualized.

Conflict of Interests

The authors declare that there is no conflict of interests regarding the publication of this paper.

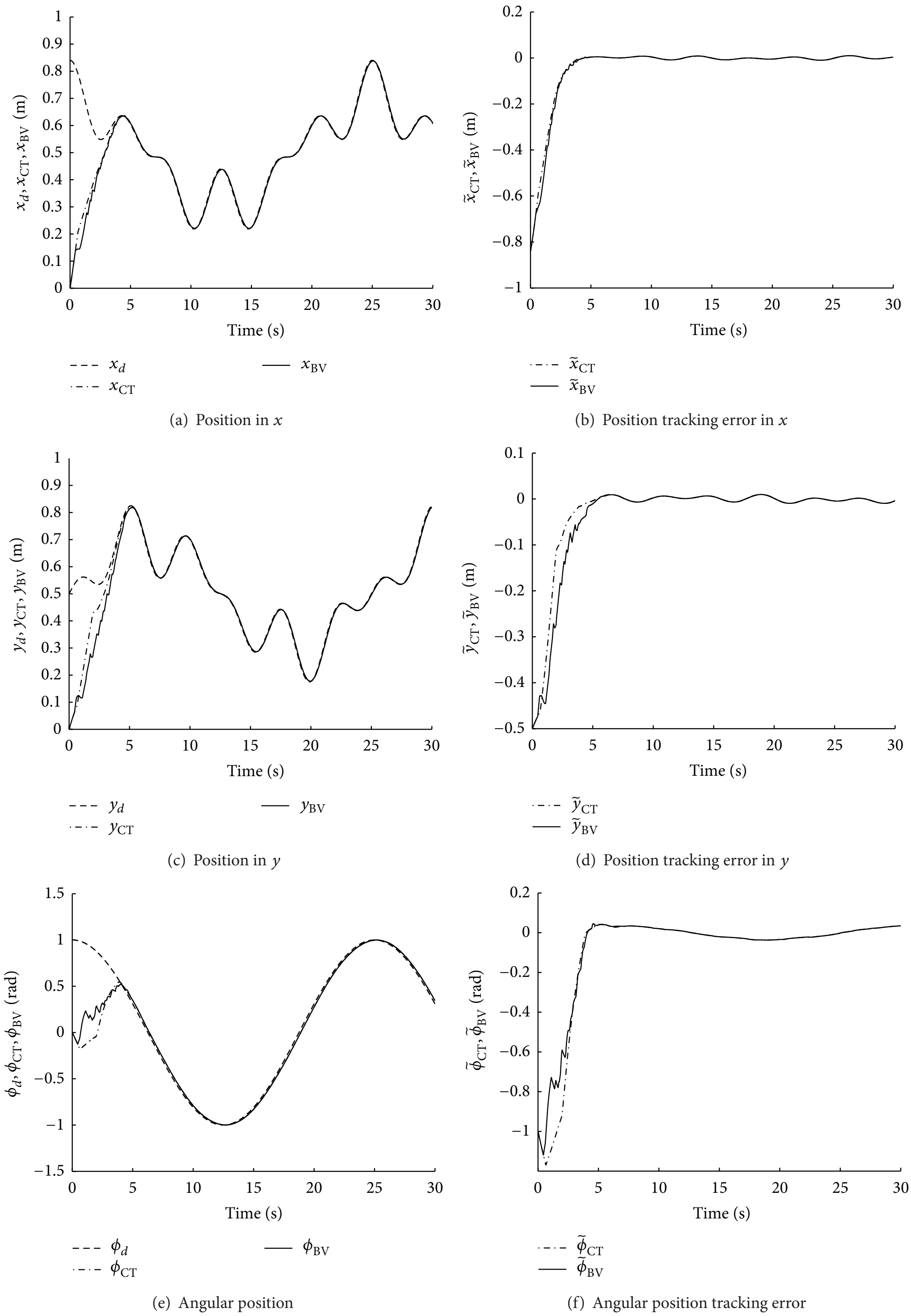

(a) Position in x

(b) Position tracking error in x

(c) Position in y

(d) Position tracking error in y

(e) Angular position

(f) Angular position tracking error

Figure 10: Experimental results of the positions and tracking errors of the OMR under the action of the CT and BV controllers.

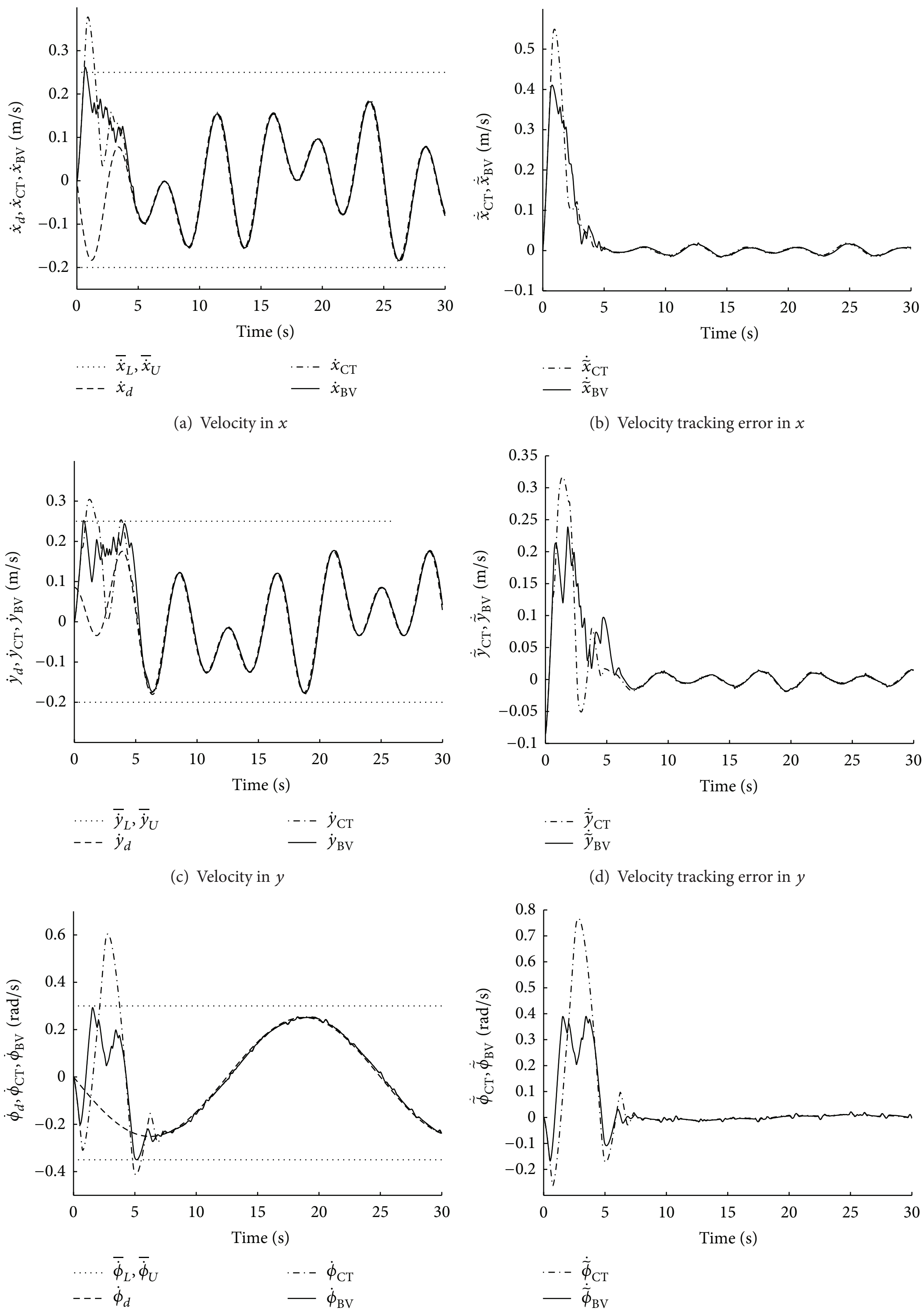

(a) Velocity in x

(b) Velocity tracking error in x

(c) Velocity in y

(d) Velocity tracking error in y

(e) Angular velocity

(f) Angular velocity tracking error

FIGURE 11: Experimental results of the velocities and tracking errors of the OMR under the action of the CT and BV controllers.

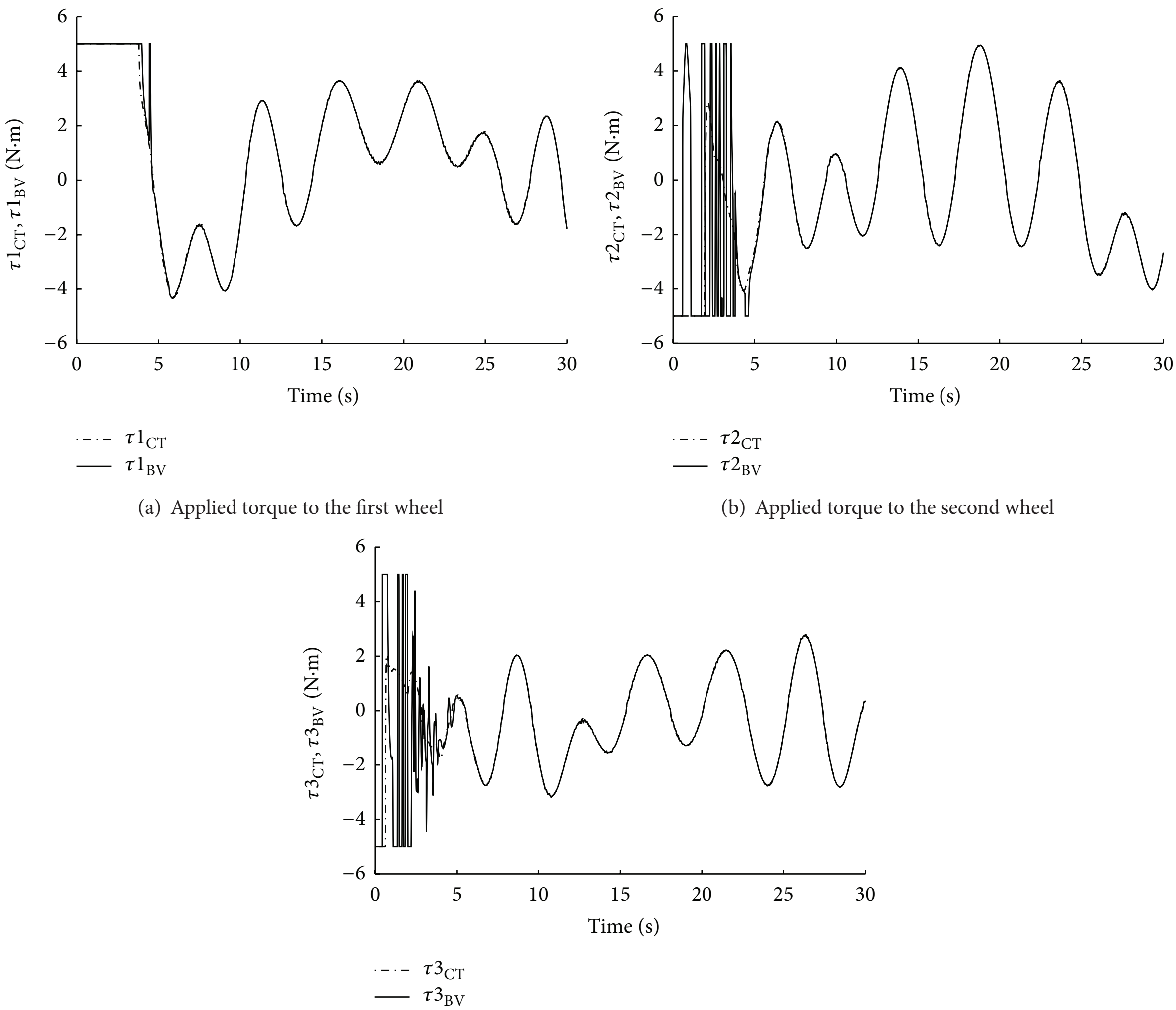

(a) Applied torque to the first wheel

(b) Applied torque to the second wheel

(c) Applied torque to the third wheel

FIGURE 12: Experimental results of the torques applied to the OMR under the action of the CT and BV controllers.

Acknowledgments

Ollin Peñaloza-Mejía acknowledges the financial support given for this work by the Instituto Tecnológico de Sonora (ITSON). Luis A. Márquez-Martínez and Joaquín Alvarez acknowledge the financial support given for this work by the National Council of Science and Technology of Mexico (CONACyT), under Grant no. CB2012-01-180011-Y. Miguel G. Villarreal-Cervantes acknowledges support from CONACyT and the Instituto Politécnico Nacional. Ramón García-Hernández thanks Universidad Autónoma del Carmen and ITSON for supporting his research stage.

References

[1] W. Dixon, D. W. Dawson, E. Zergeroglu, and A. Behal, *Nonlinear Control of Wheeled Mobile Robot*, vol. 262 of *Lectures Notes in Control and Information Sciences*, Springer, Berlin, Germany, 2001.

[2] F. G. Pin and S. M. Killough, "New family of omnidirectional and holonomic wheeled platforms for mobile robots," *IEEE Transactions on Robotics and Automation*, vol. 10, no. 4, pp. 480–489, 1994.

[3] M. W. Spong, S. Hutchison, and M. Vidyasagar, *Robot Modeling and Control*, John Wiley & Sons, 2006.

[4] Y. Liu, J. J. Zhu, J. Wu, and R. L. Williams II, "Omni-directional mobile robot controller based on trajectory linearization," *Robotics and Autonomous Systems*, vol. 56, no. 5, pp. 461–479, 2008.

[5] C. Treesatayapun, "A discrete-time stable controller for an omni-directional mobile robot based on an approximated model," *Control Engineering Practice*, vol. 19, no. 2, pp. 194–203, 2011.

[6] H. Sira-Ramírez, C. López-Uribe, and M. Velasco-Villa, "Linear observer-based active disturbance rejection control of the omnidirectional mobile robot," *Asian Journal of Control*, vol. 15, no. 1, pp. 51–63, 2013.

[7] J. Borenstein, H. R. Everett, L. Feng, and D. Wehe, "Mobile robot positioning: sensors and techniques," *Journal of Robotic Systems*, vol. 14, no. 4, pp. 231–249, 1997.

[8] J. Alvarez-Ramirez, V. Santibañez, and R. Campa, "Stability of robot manipulators under saturated PID compensation," *IEEE Transactions on Control Systems Technology*, vol. 16, no. 6, pp. 1333–1341, 2008.

[9] D. Omrčen, L. Žlajpah, and B. Nemec, "Compensation of velocity and/or acceleration joint saturation applied to redundant manipulator," *Robotics and Autonomous Systems*, vol. 55, no. 4, pp. 337–344, 2007.

[10] O. Dahl and L. Nielsen, "Torque-limited path following by online trajectory time scaling," *IEEE Transactions on Robotics and Automation*, vol. 6, no. 5, pp. 554–561, 1990.

[11] G. Antonelli, S. Chiaverini, and G. Fusco, "A new on-line algorithm for inverse kinematics of robot manipulators ensuring path tracking capability under joint limits," *IEEE Transactions on Robotics and Automation*, vol. 19, no. 1, pp. 162–167, 2003.

[12] O. Gerelli and C. G. Lo Bianco, "Nonlinear variable structure filter for the online trajectory scaling," *IEEE Transactions on Industrial Electronics*, vol. 56, no. 10, pp. 3921–3930, 2009.

[13] G. Antonelli, C. Curatella, and A. Marino, "Constrained motion planning for open-chain industrial robots," *Robotica*, vol. 29, no. 3, pp. 403–420, 2011.

[14] F. Flacco, A. de Luca, and O. Khatib, "Motion control of redundant robots under joint constraints: saturation in the null space," in *Proceedings of the IEEE International Conference on Robotics and Automation (ICRA '12)*, pp. 285–292, Saint Paul, Minn, USA, 2012.

[15] A. Loria and H. Nijmeijer, "Bounded output feedback tracking control of fully actuated Euler-Lagrange systems," *Systems and Control Letters*, vol. 33, no. 3, pp. 151–161, 1998.

[16] C. Q. Huang, X. F. Peng, C. Z. Jia, and J. D. Huang, "Guaranteed robustness-performance adaptive control with limited torque for robot manipulators," *Mechatronics*, vol. 18, no. 10, pp. 641–652, 2008.

[17] V. Santibañez, K. Camarillo, J. Moreno-Valenzuela, and R. Campa, "A practical PID regulator with bounded torques for robot manipulators," *International Journal of Control, Automation and Systems*, vol. 8, no. 3, pp. 544–555, 2010.

[18] L. G. van Willigenburg, "Computation and implementation of digital time-optimal feedback controllers for an industrial X-Y robot subjected to path, torque, and velocity constraints," *International Journal of Robotics Research*, vol. 12, no. 5, pp. 420–433, 1993.

[19] M. Danesh, F. Sheikholeslam, and M. Keshmiri, "Robust robot controller design using joint position and velocity dependent uncertainty bound," in *Proceedings of the IEEE/RSJ International Conference on Intelligent Robots and Systems (IROS '06)*, Beijing, China, October 2006.

[20] R. Kikuuwe, T. Yamamoto, and H. Fujimoto, "Velocity-bounding stiff position controller," in *Proceedings of the IEEE/RSJ International Conference on Intelligent Robots and Systems (IROS '06)*, pp. 3050–3055, Beijing, China, October 2006.

[21] K. B. Ngo and R. Mahony, "Bounded torque control for robot manipulators subject to joint velocity constraints," in *Proceedings of the IEEE International Conference on Robotics and Automation (ICRA '06)*, pp. 7–12, Orlando, Fla, USA, May 2006.

[22] X. Papageorgiou and K. J. Kyriakopoulos, "Compliant motion tasks for robot manipulators subject to joint velocity constraints," in *Proceedings of the 47th IEEE Conference on Decision and Control (CDC '08)*, pp. 4570–4575, IEEE, Cancún, Mexico, December 2008.

[23] C. G. L. Bianco and O. Gerelli, "Online trajectory scaling for manipulators subject to high-order kinematic and dynamic constraints," *IEEE Transactions on Robotics*, vol. 27, no. 6, pp. 1144–1152, 2011.

[24] F. Garelli, L. Gracia, A. Sala, and P. Albertos, "Sliding mode speed auto-regulation technique for robotic tracking," *Robotics and Autonomous Systems*, vol. 59, no. 7-8, pp. 519–529, 2011.

[25] F. Flacco and A. de Luca, "Optimal redundancy resolution with task scaling under hard bounds in the robot joint space," in *Proceedings of the IEEE International Conference on Robotics and Automation (ICRA '13)*, pp. 3969–3975, Karlsruche, Germany, May 2013.

[26] J. F. Guerrero-Castellanos, M. G. Villarreal-Cervantes, J. P. Sánchez-Santana, and S. Ramírez-Martínez, "Seguimiento de trayectorias de un robot móvil (3,0) mediante control acotado," *Revista Iberoamericana de Automática e Informática Industrial*, vol. 11, no. 4, pp. 426–434, 2014.

[27] V. Sankaranarayanan and A. D. Mahindrakar, "Configuration constrained stabilization of a wheeled mobile robot—theory and experiment," *IEEE Transactions on Control Systems Technology*, vol. 21, no. 1, pp. 275–280, 2013.

[28] R. Oftadeh, R. Ghabcheloo, and J. Mattila, "A novel time optimal path following controller with bounded velocities for mobile robots with independently steerable wheels," in *Proceedings of the 26th IEEE/RSJ International Conference on Intelligent Robots and Systems (IROS '13)*, pp. 4845–4851, IEEE, Tokyo, Japan, November 2013.

[29] K. D. Do, "Bounded controllers for global path tracking control of unicycle-type mobile robots," *Robotics and Autonomous Systems*, vol. 61, no. 8, pp. 775–784, 2013.

[30] T. A. Jesus, L. C. A. Pimenta, L. A. B. Tôrres, and E. M. A. M. Mendes, "Consensus for double-integrator dynamics with velocity constraints," *International Journal of Control, Automation and Systems*, vol. 12, no. 5, pp. 930–938, 2014.

[31] Y. Zhang, W. Li, and Z. Zhang, "Physical-limits-constrained minimum velocity norm coordinating scheme for wheeled mobile redundant manipulators," *Robotica*, 26 pages, 2014.

[32] H. K. Khalil, *Nonlinear Systems*, Prentice Hall, New York, NY, USA, 3rd edition, 2002.

[33] B. Brogliato, R. Lozano, B. Maschke, and O. Egeland, *Dissipative Systems Analysis and Control: Theory and Applications*, Springer, 2nd edition, 2007.

[34] V. Utkin, J. Guldner, and J. Shi, *Sliding Mode Control in Electro-Mechanical Systems*, Automation and Control Engineering Series, CRC Press, Boca Raton, Fla, USA, 2nd edition, 2009.

[35] M. G. Villarreal-Cervantes, C. A. Cruz-Villar, J. Álvarez-Gallegos, and E. A. Portilla-Flores, "Kinematic dexterity maximization of an omnidirectional wheeled mobile robot: a comparison of metaheuristic and SQP algorithms," *International Journal of Advanced Robotic Systems*, vol. 9, no. 161, pp. 1–7, 2012.

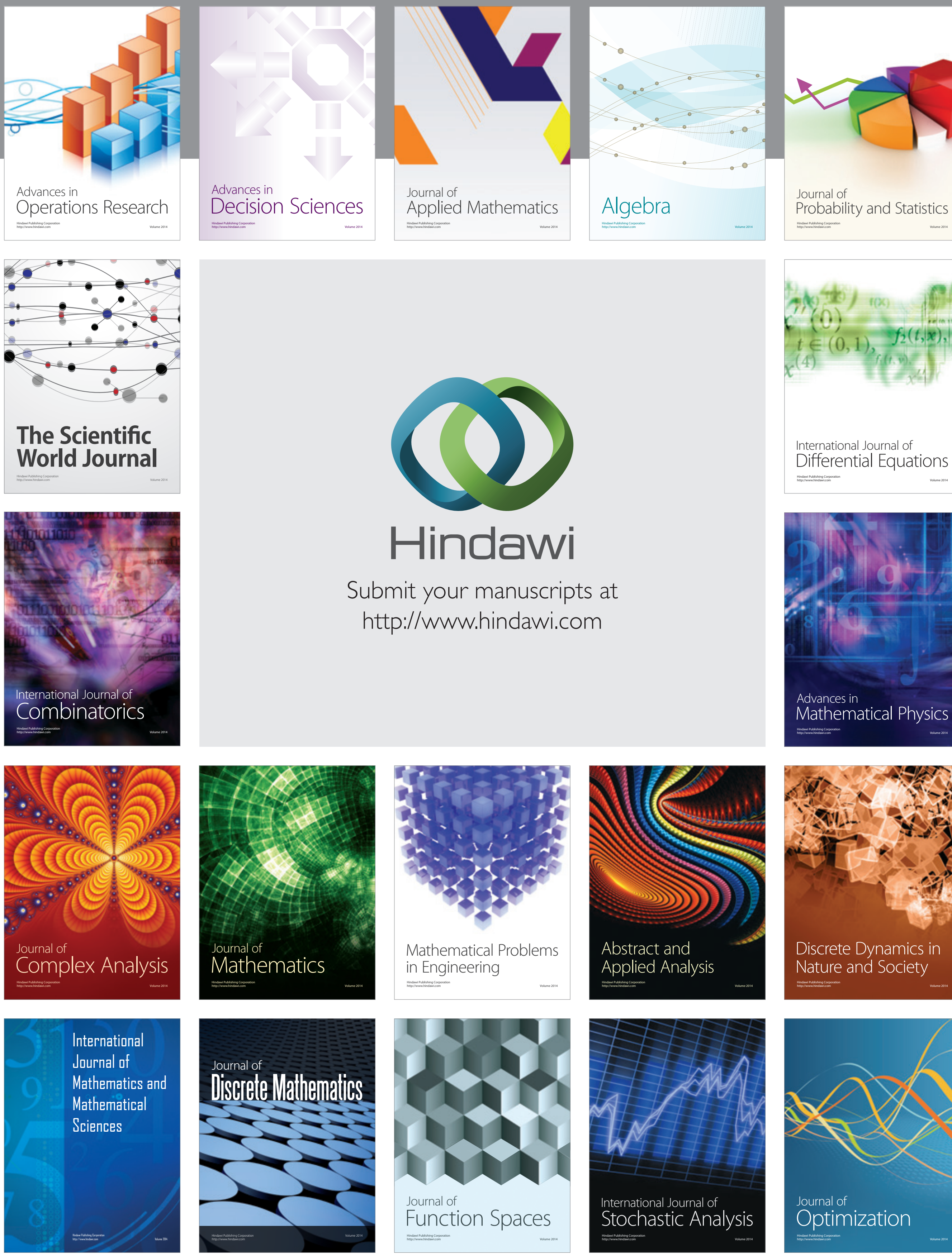

Advances in
Operations Research
Advances in
Decision Sciences
Journal of
Applied Mathematics
Algebra
Journal of
Probability and Statistics
The Scientific
World Journal
International Journal of
Differential Equations
Hindawi
Submit your manuscripts at
http://www.hindawi.com
International Journal of
Combinatorics
Advances in
Mathematical Physics
Journal of
Complex Analysis
Journal of
Mathematics
Mathematical Problems
in Engineering
Abstract and
Applied Analysis
Discrete Dynamics in
Nature and Society
International
Journal of
Mathematics and
Mathematical
Sciences
Journal of
Discrete Mathematics
Journal of
Function Spaces
International Journal of
Stochastic Analysis
Journal of
Optimization